Journal of Petroleum Science and Engineering 182 (2019) 106363

Contents lists available at ScienceDirect

Journal of Petroleum Science and Engineering

journal homepage: www.elsevier.com/locate/petrol

# Fractal characteristics of the pore structures of fine-grained, mixed sedimentary rocks from the Jimsar Sag, Junggar Basin: Implications for lacustrine tight oil accumulations

Jian Wang[a,b,*], Yingchang Cao[a,b,**], Keyu Liu[a,b,c], Yang Gao[d], Zhijun Qin[d]

[a] School of Geosciences, China University of Petroleum (East China), Qingdao 266580, China
[b] Key Laboratory of Deep Oil & Gas Geology and Geophysics (China University of Petroleum), Ministry of Education, Qingdao 266580, China
[c] Department of Applied Geology, Curtin University, GPO Box U1987, Perth, WA 6845, Australia
[d] Research Institute of Petroleum Exploration and Development, PetroChina Xinjiang Oilfield, Karamay 841000, China

ARTICLE INFO

*Keywords:*
Fractal dimension
Mixed sedimentary rock
Nanopore
Tight oil
Permian
Junggar Basin

ABSTRACT

The tight reservoir property and oil accumulation are greatly affected by the complexity and heterogeneity of pore structure. Fine-grained, mixed sedimentary formation samples from the Permian Lucaogou Formation in the Jimsar Sag were systematically studied focusing on their fractal characteristics and effects on the storage space, minerals and diagenesis, and its implication for tight oil accumulation. Fractal dimensions were calculated by the MICP model equation. The lacustrine fine-grained, mixed sedimentary samples are characterized by single and multi-fractal structures. Compared with the multi-fractal reservoir, the pore-throat structure of single fractal reservoir is more uniform and the pore throat size is relatively smaller. Minerals and diagenesis have apparent influences on fractal characteristics of the lacustrine MSR tight oil reservoir. The enrichment of terrestrial minerals can increase the heterogeneity of storage space and might be the reason for the multi-fractal pore structures. The enrichment of tuff in mixed sedimentary rock (MSR) can greatly improve the property and reduce the fractal dimension of tight reservoirs through dissolution. Large-pore filling calcite has dual effects on destroying reservoir space and reducing heterogeneity, which makes the weak correlation between calcite and fractal dimension. Fractal characteristics implicate that pore structures play a very significant role in controlling the accumulation of tight oil. MSRs with $D$ or $D_e$ more than 2.586 and porosity (average pore-throat radius) less than 6.3% (0.05 μm) are mostly incapable of effectively accumulating oil.

## 1. Introduction

Unconventional oil and gas resources have become an important inventory of fossil fuels in the world (Zou et al., 2012, 2013). Tight oil has become an important field of unconventional oil and gas exploration and development because of its rich reserves, wide distribution and high reliability of recoverable resources (Zou et al., 2013; Ghanizadeh et al., 2015; Ma et al., 2015). Different from conventional reservoirs, tight oil reservoirs are dominated by extremely heterogeneous reservoirs with nanoscale pore systems with small pore-throat size and complex pore-throat structure, which controls oil accumulation and percolation ability (Loucks et al., 2009, 2017; Shanley and Cluff, 2015; Wang et al., 2019). Because the pore structure of tight oil reservoirs is extremely complex, conventional petrophysical parameters (e.g., porosity and permeability) cannot effectively characterize the tight oil reservoir properties (Lai and Wang, 2015; Wang et al., 2018a). Scanning electron microscopy (SEM) (Barnard et al., 2012; Chalmers et al., 2012), image analysis of thin section (Carr et al., 1996), X-ray CT (Bai et al., 2013), mercury injection (Clarkson et al., 2013; Zhao et al., 2015), gas adsorption (Clarkson et al., 2012, 2013) and nuclear magnetic resonance (NMR) (Carr et al., 1996) are often used to analyze pore-throat structures of tight oil reservoirs by obtaining parameters of pore-throat size, connectivity, and sorting (Anovitz et al., 2013; Shanley and Cluff, 2015; Zhao et al., 2015; Sharawy and Gaafar, 2019). However, these analytical methods often have different standards (Cao et al., 2016a; Chen et al., 2016), and are affected by the inconsistency between the parameters of planar geometry model and the actual application (Cao et al., 2016a; Yang et al., 2016), the obtained pore-throat structure parameters cannot fully reflect the strong heterogeneity of tight oil reservoirs (Cao et al., 2016a; Chen et al., 2016; Yang et al.,

* Corresponding author. No. 66 West Changjiang Rd., Huangdao District, Qingdao, China.
** Corresponding author. No. 66 West Changjiang Rd., Huangdao District, Qingdao, China.
*E-mail addresses:* wangjian8601@upc.edu.cn (J. Wang), caoych@upc.edu.cn (Y. Cao).

https://doi.org/10.1016/j.petrol.2019.106363
Received 12 January 2019; Received in revised form 2 July 2019; Accepted 8 August 2019
Available online 09 August 2019
0920-4105/ 

2016).

Since the founding of fractal geometry, fractal dimension has become an important parameter for quantitatively describing microscopic pore structures and their combination characteristics (Mandelbrot et al., 1984; Cao et al., 2016a; Chen et al., 2016; Yang et al., 2016). Fractal theory describes the complexity and heterogeneity of pore surface or pore structure by self-similarity (Pfeifer et al., 1989; Jaroniec, 1995; Wang et al., 2015a; Xu et al., 2018). In 3D Euclidean space, the fractal dimension of pore structure is between 2 and 3. The larger the fractal dimension, the rougher the pore surface is, the stronger the heterogeneity is, and the worse the reservoir property would be (Pfeifer and Avnir, 1983; Wang et al., 2015b; Yang et al., 2016; Fu et al., 2017; Mendhe et al., 2017; Shao et al., 2017). Previous fractal studies of pore structures often focused on shale (Cao et al., 2016a; Chen et al., 2016; Yang et al., 2016; Wang et al., 2015a; Shao et al., 2017), coal (Mahamud and Novo, 2008; Fu et al., 2017; Mendhe et al., 2017), tight sandstone (Li et al., 2017) and tight carbonate (Xu et al., 2018) reservoirs and achieved good results.

Junggar Basin is an important and famous hydrocarbon-bearing basin in northwestern China, which contains abundant tight oil resources. In recent years, many important breakthroughs have been made in tight oil exploration and development of the Lucaogou Formation in the Jimsar Sag, Junggar Basin, which has become a model for successful exploration and development of tight oil in China (Cao et al., 2016b; Wu et al., 2016). The notable characteristic of the tight oil reservoir in the Jimsar Sag is mixed sedimentary rock (MSR) composed of terrigenous clast, dolomite and tuff, which is distinctly different from the reported lacustrine or marine MSRs composed of terrigenous clast and siliceous/carbonate (Myrow and Landing, 1992; Palermo et al., 2008). The particularity of the composition of the MSR inevitably leads to the unique and complex reservoir pore structure characteristics. Lacustrine tight oil reservoirs in many areas are very similar to the Lucaogou Formation in the Jimsar Sag, such as the Fengcheng Formation in the Mahu Sag of the Junggar Basin (Tao et al., 2016), the Tiaohu Formation in the Santanghu Basin (Ma et al., 2015, 2019), the Tengger Formation in the Erlian Basin (Wei et al., 2017). Therefore, the study on pore structure of the tight oil reservoir of the Lucaogou Formation is not only of great academic significance for understanding reservoir characteristics of the specific MSR reservoirs, but also has a good reference significance for analyzing similar tight oil reservoirs in other basins. But at present, pore throat structure and reservoir heterogeneity are mainly described by storage space and pore-throat parameters (Ma et al., 2018; Su et al., 2018), which are difficult to fully explain reservoir properties. In order to comprehensively understand the pore structures of the MSR reservoir, the fractal characteristics of pore structures was determined by using mercury injection capillary pressure (MICP) data to better characterize the reservoir pore structures. The fractal dimensions were correlated with the nanopore parameters and mineral contents, which were determined using Helium porosimetry, MICP, XRD, microscopy, SEM and carbon and oxygen isotope to clarify the controls of mineral compositions and diagenesis. Finally, combined with oil-bearing analysis, the implications of the fractal characteristics of the pore structures on the tight oil accumulation was determined.

## 2. Geological background

Junggar Basin is an important hydrocarbon-bearing basin in the NW China (Fig. 1A), which has great oil and gas resources and exploration potential. The Jimsar Sag, with the area is 1278 $km^2$, is an important oil-rich sag in the east of the Junggar Basin (Fig. 1B). It is bordered by the Jimsar fault and the Shaqi uplift in the north, the Xidi fault and the Laozhuangwan fault in the west, the Santai fault in the south, and the Qitai uplift in the east (Fig. 1C). The Jimsar Sag has undergone multistage tectonic movements since the Hercynian movement on the basement of the Carboniferous igneous rock, and deposited Permian, Triassic, Jurassic, Cretaceous, Paleogene, Neogene and Quaternary (Ding et al., 2017). The stratum thickness has gradually decreased from west to east (Fig. 1C). The Permian Lucaogou Formation is mainly composed of semi-deep to deep lake deposits with the characteristics of large thickness and wide area and is the main source rock in the sag. The favorable area with thickness greater than 200 m is up to 806 $km^2$. The Lucaogou Formation, with the thickness is 200–300m, is the main tight oil production layer. The Lucaogou Formation is dominated by the fine-grained MSR due to the complex and diverse rock compositions (Fig. 1D).

## 3. Methodology

Eighty-eight core samples of fine-grained MSR were collected from 5 wells in the study area (Fig. 1C). In order to effectively identify pore space, blue resin was injected into samples before thin sectioning. Alizarin Red S and K-ferricyanide were dyed on thin sections partly to determine carbonate minerals. Ten samples were analyzed by ZEISS SEM under the conditions of 20 °C, 35%RH, and 20.0 kV.

Cylinders with diameters of 2.5 cm were drilled down from the cores and used to measure the pore volume and pore-throat parameters through the mercury injection. The maximum mercury injection pressure is 163.84 MPa. According to Boyle's law, the porosity was measured using a helium porosimeter following the process of Wang et al. (2018b). Mineralogical compositions of fifty samples were analyzed through X-ray diffraction (XRD) following the method of Wang et al. (2018b). Fifty-five samples were collected for carbon and oxygen isotopes analyses using a Finnigan Mat 250 mass spectrometer under the reaction method of Al-Asam et al. (1990). The sample pretreatment method was after Wang et al. (2016). The precisions of the carbon and oxygen isotope ratios were ± 0.2‰ and ± 0.3‰, respectively.

## 4. Results and discussion

### 4.1. Fractal theory and fractal dimensions

The structure and fractal characteristics of reservoirs can be studied by many techniques and models such as HR-SEM (Krohn, 1988; Schieber, 2010), MICP (Clarkson et al., 2013; Mastalerz et al., 2013; Li et al., 2014), gas adsorption (Mastalerz et al., 2013), FIB-SEM (Curtis et al., 2012), Langmuir models (Ji et al., 2016), fractal Frenkel − Halsey − Hill (FHH) models (Pfeifer et al., 1989; Xu et al., 2018), the thermodynamic method (Pfeifer et al., 1989), image qualitative evaluations (Dathe et al., 2001), LTNA (Fu et al., 2017; Shao et al., 2017), and NMR (Zhou et al., 2016). Because the mercury intrusion method can directly measure pore distribution characteristics of samples from inside, MICP using wetting phase saturation data has become the most important method to measure and calculate fractal dimension (Clarkson et al., 2013; Mastalerz et al., 2013; Li et al., 2014; Lai and Wang, 2015; Zhao et al., 2015). The published MICP model equation can be used to calculate the fractal dimension (Lai and Wang, 2015; Li et al., 2017).

$$\lg S_w = (D - 3)\lg p_c + (3 - D)\lg p_{min} \quad (1)$$

where $S_w$ represents the wetting phase fluid saturation (%), $p_c$ represents capillary pressure (MPa), $p_{min}$ represents breakthrough capillary pressure (MPa), and $D$ represents the fractal dimension. The fractal dimension $D$ can be calculated from the line slope under the condition of pore fractal through eq. (1).

The lacustrine fine-grained MSR samples have single and multi-fractal structures (Fig. 2). Only a good linear relationship between $\lg p_c$ and $\lg S_w$ in the single fractal structure (Fig. 2A). The correlations ($R^2$) are in the range of 0.9756–0.9942 (av. 0.9901). The high $R^2$ suggests that lacustrine fine-grained MSR samples with single fractal structure have continuous pore diameter and consistent fractal characteristics in different pore sizes (Pfeifer et al., 1989; Mastalerz et al., 2013; Li et al., 2014; Xu et al., 2018). Uniformly mercury intrusion curves of the lacustrine fine-grained MSR samples with single fractal structure also

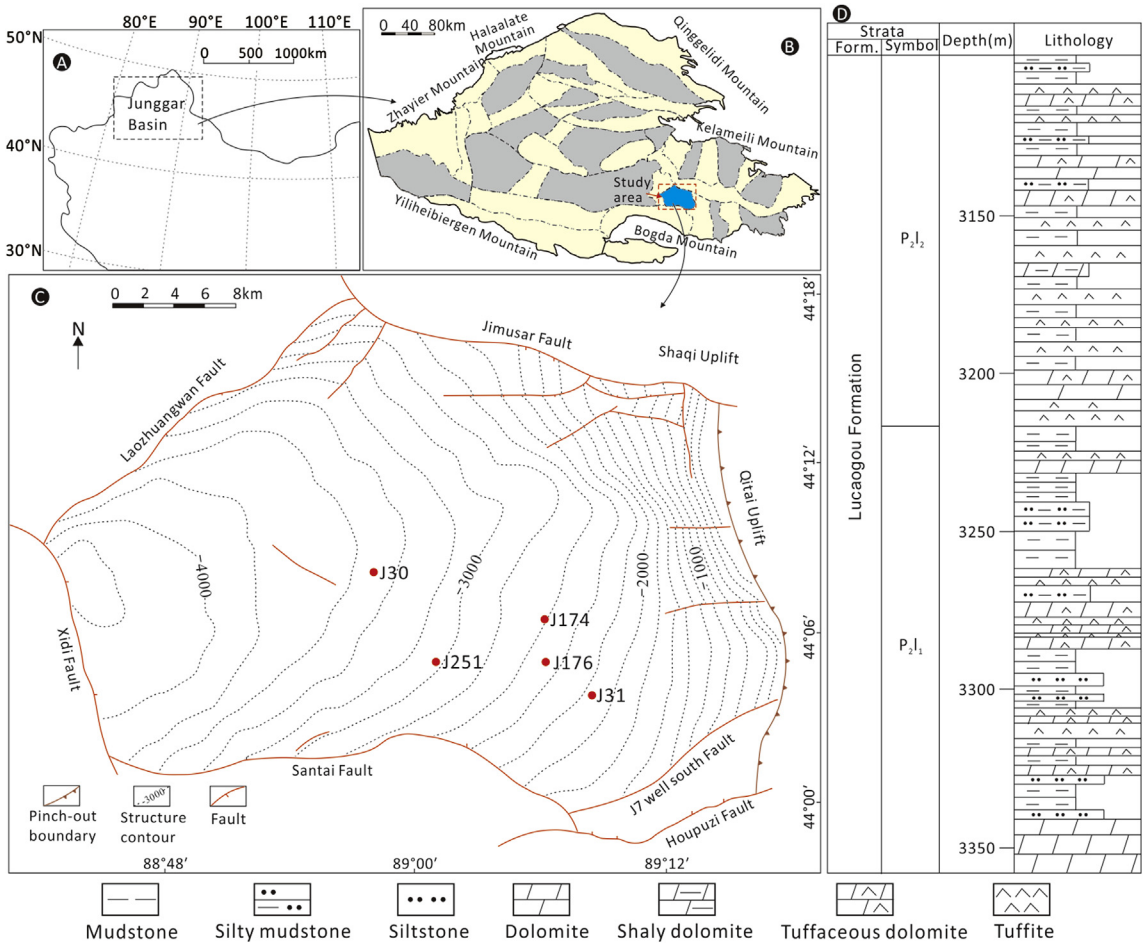


**Fig. 1.** (A) Location of the Junggar Basin in the northwestern China; (B) Tectonic position of the Jimsar Sag; (C) Structure-contour map of the top surface of the Lucaogou Formation and sampling wells in the Jimsar Sag; (D) Summary lithostratigraphy (well J-174) of the Lucaogou Formation in the Jimsar Sag (Modified after Ding et al., 2017). Form.-Formation.

indicate the continuous pore diameter and consistent fractal characteristics (Fig. 2B). The fractal dimension $D$ of the single fractal samples is between 2.1972 and 2.8838.

Two different gradients with good correlations lg $p_c$ and lg $S_w$ exist in the multi-fractal structures (Fig. 2 C). The turning points of $p_c$ of the two different gradients are mainly between 5.12 MPa and 20.48 MPa. The correlations ($R^2$) of the curves of lg $p_c$ vs. lg $S_w$ for the $D_1$ are between 0.9802 and 0.9954 with an average 0.9915, the correlations ($R^2$) for $D_2$ are between 0.9668 and 0.9918 with an average 0.9874. The high $R^2$ indicate that the lacustrine fine-grained MSR samples with multi-fractal structure have the dividing pore diameter and different fractal characteristics in different pore sizes (Krohn, 1988; Dathe et al., 2001; Schieber, 2010; Curtis et al., 2012; Mastalerz et al., 2013; Li et al., 2014; Lai and Wang, 2015; Ji et al., 2016; Zhou et al., 2016; Xu et al., 2018). The corresponding mercury intrusion curves also have obvious inflection points (Fig. 2D). The fractal dimension $D_1$ and $D_2$ of the multi-fractal samples are 2.0071–2.817 and 2.8319–2.9327, respectively, suggesting that the heterogeneity of large pores is stronger than that of relatively small pores, which is inconsistent with previous studies on shale and lacustrine carbonates (Wang et al., 2015a,b; Yang et al., 2016; Xu et al., 2018).

### 4.2. Relationships between fractal characteristics and nanopore parameters

Though the frequency of the average pore-throat radius of the single fractal and multi-fractal samples are similar, the contents of the average pore-throat radius < 0.05 μm and > 0.2 μm of multi-fractal samples are higher than those of single fractal samples, the content of the average pore-throat radius between 0.05μm and 0.2 μm of multi-fractal samples is lower than that of single fractal samples (Fig. 3). The pore-throat size of the single fractal samples is more uniform and concentrated than that of the multi-fractal samples.

For single fractal samples, the fractal dimension $D$ have negative correlations with porosity and average pore-throat radius and positive correlations with sorting coefficient and ratio of pore and throat volumes (Fig. 4), indicating that the storage spaces and pore-throat sizes increase and the sorting and pore-throat connectivity become better with the decreasing fractal dimension $D$ (Pfeifer and Avnir, 1983; Yang et al., 2016; Fu et al., 2017; Mendhe et al., 2017; Shao et al., 2017). For multi-fractal samples, the fractal dimension $D_1$ and $D_2$ have negative correlation with contribution of mercury saturation (Fig. 5). The contributions of mercury saturation of small pores and relatively large pores are between 59.5% and 89.6% (av. 76%) and 10.4%–40.5% (av. 24%), respectively, indicating the reservoir space of the lacustrine fine-grained, MSR is dominated by small pores. The $D_1$ has negative correlations with porosity and average pore-throat radius and positive correlations with ratio of pore and throat volumes and sorting coefficient (Fig. 4C and D). Similar to the characteristics of single fractal samples, the good sorting, smoothness of pore surface and connectivity of pore-throat of the dominated small pores are conducive to the development of high reservoir space and large pore-throat (Mahamud and Novo, 2008; Chen et al., 2016; Yang et al., 2016; Fu et al., 2017; Li et al., 2017; Mendhe et al., 2017; Shao et al., 2017). The $D_2$ negatively correlated with porosity, average pore-throat radius and sorting

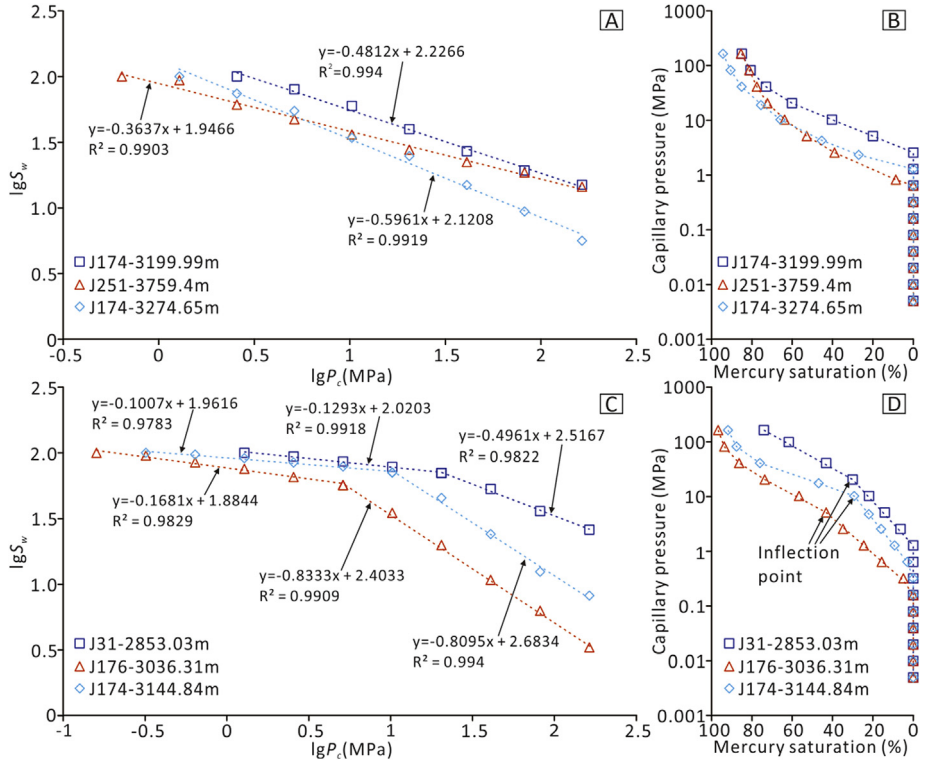


**Fig. 2.** Typical plots of lg $p_c$ versus lg $S_w$ from the MICP model using the wetting phase saturation data and corresponding mercury intrusion curves.

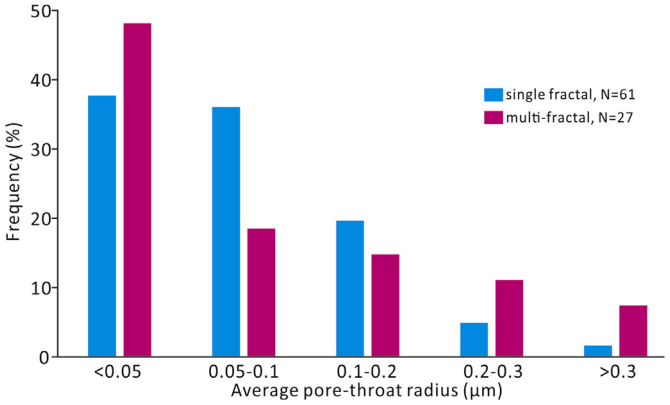


**Fig. 3.** Frequency of average pore-throat radius of lacustrine fine-grained MSR samples with single and multi-fractal.

coefficient, and has no obvious relationship with the ratio of pore and throat volumes (Fig. 4), suggesting that the relatively large pores with low content has poor connectivity and sorting and has weak influence on storage space, which can interpret why the fractal dimension of large pores is higher than that of small pores.

For multi-fractal samples, the entire fractal dimension ($D_e$) of one sample can be calculated by the weighted mean of local fractal $D_1$ and $D_2$ using the contribution of mercury saturation as weight coefficient (Li et al., 2017). The $D_e$ of the multi-fractal samples is between 2.1035 and 2.8402, with an average of 2.4398. The correlations between $D_e$ and nanopore parameters of multi-fractal samples are similar to that of $D_1$ (Fig. 4), which can also indicate the relatively large pores has weak influence on storage space and explain the higher fractal dimension of large pores.

### 4.3. Effects of minerals on fractal characteristics

The lacustrine fine-grained MSR mainly consists of quartz, feldspar (mainly plagioclase and K-feldspar), carbonate (mainly dolomite and calcite) and clay minerals (Fig. 6). The contents of minerals are shown in Table 1. Quartz and clay are typical terrigenous minerals (Fig. 6A, B, F), dolomite and calcite are authigenic minerals (Fig. 6 B, C, D, E), and feldspar mainly includes feldspar in tuff (Fig. 6A), authigenic albite (Fig. 6C, D) and a small amount of terrigenous (Fig. 6A and B) (Ma et al., 2018; Su et al., 2018). Authigenic albite is mainly from the hydrolysis and dissolution of tuff (Su et al., 2018). Therefore, the content of feldspar can reflect the content of tuff. The minerals in lacustrine fine-grained MSR have strong effects on fractal characteristics (Fig. 7). For single fractal samples, the terrigenous quartz and clay and the authigenic dolomite are positively related with $D$ (Fig. 7A, B, C) and the calcite has no obvious influence on $D$ (Fig. 7D), whereas feldspars are negatively correlated with $D$ (Fig. 7E and F), indicating that the quartz, clay and dolomite are propitious to increase the $D$ values, whereas the feldspars are in favor of decreasing the $D$ value. For multi-fractal samples, correlations between quartz, clay, carbonate and feldspar and $D_1$, $D_2$ and $D_e$ are similar to those of single fractal samples (Fig. 7). Correlations between minerals and $D_1$ are better than that of $D_2$ (Fig. 7), indicating that minerals mainly affect the $D_1$ value, but have little effect on $D_2$ value.

The above discussion indicates that terrigenous minerals, authigenic minerals and minerals in tuff all have great impact on the fractal characteristics of the lacustrine fine-grained MSR reservoirs, which are related to the particularity of the lake environment (Ding et al., 2017; Yang et al., 2019). Influenced by the Hercynian movement, the uplift of the Bogda Mountains makes the Jimsar Sag become a closed foreland lake basin at the end of the early Permian (Wang et al., 2018a,b,c). The good correlation between $\delta^{13}C$ and $\delta^{18}O$ ($R^2$ = 0.6843) also indicates the close lake of the Lucaogou Formation (Fig. 8; Talbot, 1990). In addition, the carbon isotope values are in the range of non-fresh water carbonates (Keith and Weber, 1964; Wang et al., 2018c), indicating the saline sedimentary environment. A large amount of dolomites have been formed under the depositional conditions of saline and close lake, which can support their strong impact on the fractal characteristics of nanopore structures. Due to the closed lake environment, the supply of

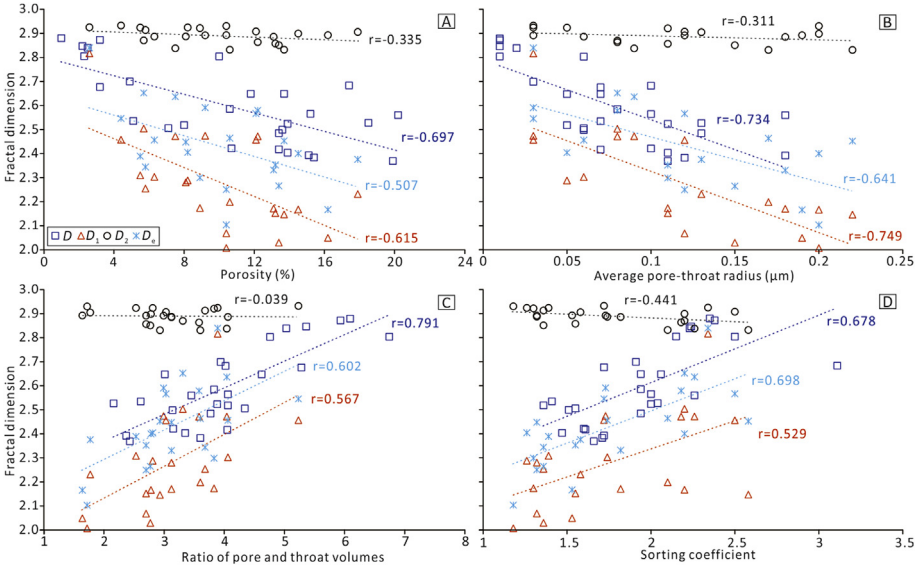


**Fig. 4.** Correlations between fractal dimensions and nanopore parameters of the lacustrine fine-grained MSR samples with single and multi-fractal.

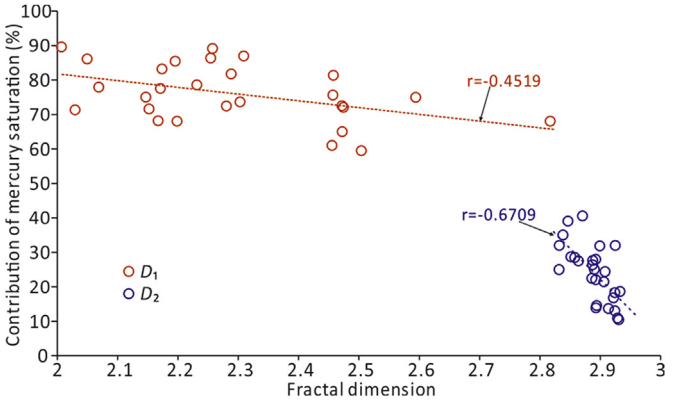


**Fig. 5.** Correlations between fractal dimension $D_1$ and $D_2$ and contribution of mercury saturation of the lacustrine fine-grained MSR samples with multi-fractal.

terrestrial minerals is relatively small. Only a small amount of samples of carbon and oxygen isotope values are consistent with terrigenous lakes also illustrate the limited terrestrial mineral intrusion (Fig. 8). Though the amount of terrestrial minerals was not enough to restrain the formation of carbonates (Fig. 9), the terrestrial minerals usually have local enrichment characteristics in lacustrine fine-grained MSR (Ma et al., 2018; Yang et al., 2019), which can apparently influence the fractal characteristics of nanopore structures (Fig. 7A). Content of terrestrial minerals in multi-fractal samples is higher than that in single fractal samples (Table 1), indicating that the enrichment of terrestrial minerals can increase the heterogeneity of storage space and result in multi-fractal. During the depositional period of the Lucaogou Formation the volcanic activity around the Jimsar Sag was strong due to the Tianshan orogeny (Wang et al., 2018c; Yang et al., 2019), which provided large amounts of feldspar dominated tuff to affect the fractal characteristics. The negative relationship between contents of feldspar and dolomite indicated that the volcanic activity and accumulation of tuff can change the depositional environment and prevent the formation of dolomite (Fig. 9). This is why feldspar and dolomite and terrestrial minerals have different effects on fractal characteristics of nanopore structures.

### 4.4. Effects of diagenesis on fractal characteristics

Unlike conventional shale, tight sandstone or coal, MSR has different material sources and complex mineral compositions, which can lead to various diagenesis during the burial process. On the basis of polarized light microscopy and SEM observations, it is easily found that the reservoir storage space and reservoir properties were strongly influenced by compaction (Fig. 10A and B), pressure-solution (Fig. 10C), dissolution (tuff (Fig. 6A, C, D and Fig. 10D and E), feldspar (Fig. 10F and G) and carbonate (Figs. 6E and 10H, I), cementation (carbonate (Figs. 6B and 10A, H), clay (Fig. 6F), authigenic albite (Fig. 6 C, D and Fig. 10E) and authigenic quartz (Fig. 10J), dolomitization (Fig. 10K) and recrystallization (Fig. 10L). As mentioned in section 4.2, there are good relationships between the fractal dimensions and nanopore storage spaces (porosity, average pore-throat radius) and their homogeneity (ratio of pore and throat volumes, sorting coefficient). Therefore, the effects of diagenesis on fractal dimensions can be studied by effects of different diagenesis on nanopore storage spaces and their homogeneity (Xu et al., 2018).

#### 4.4.1. Compaction and pressure-solution

The increasing compaction caused the grains to change from point contact to line contact and concave-convex contact (Fig. 10A) or made particles directional arrangement (Fig. 10B) with the increasing burial depth, which reduced storage spaces to a great extent and increased the fractal dimensions. Suture lines formed by pressure-solution (Fig. 10C) increased the reservoir heterogeneity and the fractal dimensions (Xu et al., 2018).

#### 4.4.2. Dissolution

Dissolution in the lacustrine fine-grained MSR was mainly caused by acidic fluid, including organic acid and $CO_2$ (Ma et al., 2018; Su et al., 2018). Tuff contains a large number of soluble components (mainly feldspar). Under the action of organic acid and $CO_2$, a large number of pores are formed by strong dissolution, which greatly increases the reservoir storage space (Fig. 6A, C, D and Fig. 10D and E). The dissolution of tuff is often accompanied by the formation of authigenic albite crystals (Fig. 6 C, D and Fig. 10E; Su et al., 2018). Intragranular dissolution pores can also be seen in terrigenous clastic feldspar (Fig. 10F and G). Therefore, the enrichment of feldspar minerals represents a strong dissolution, which can improve the storage space and reduce the fractal dimensions (Fig. 7E and F). Comprehensive analyses of effects of minerals and diagenesis on fractal characteristics indicate

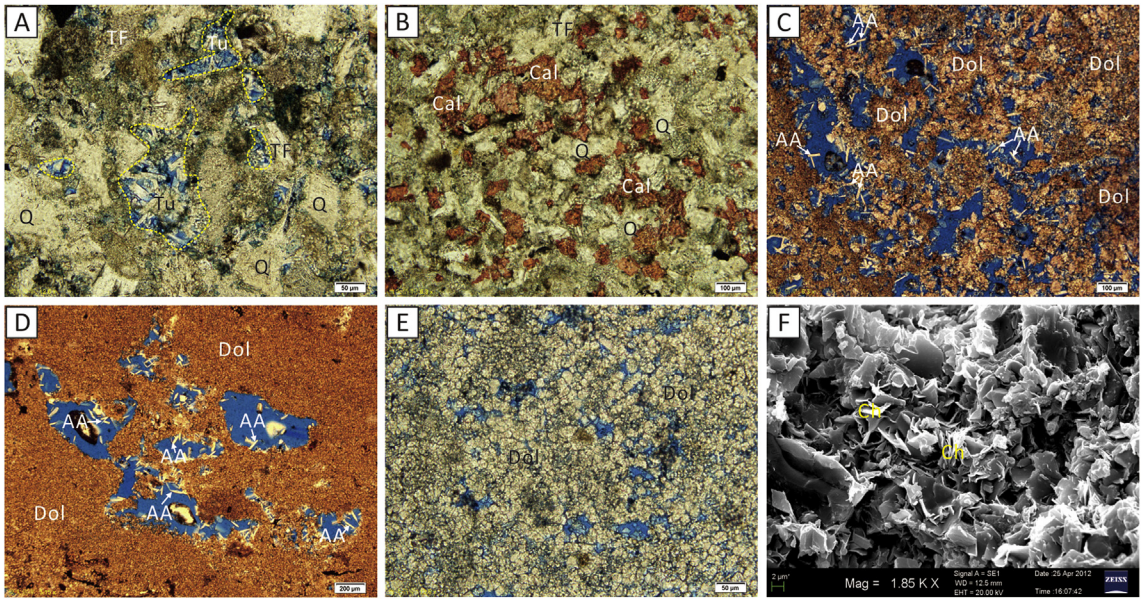


**Fig. 6.** Major minerals in lacustrine fine-grained MSR from the Lucaogou Formation of the Jimsar Sag. (A) Well J-174, 3141.04m, terrigenous quartz and feldspar and tuff with plagioclase feldspars (−). (B) Well J-174, 3199.75m, terrigenous quartz and feldspar and calcite filling in pores (−). (C) Well J-174, 3121.38m, argillaceous dolomite and authigenic albite filling pores (−). (D) Well J-174, 3155.95m, argillaceous dolomite and authigenic albite filling pores (−). (E) Well J-174, 3134.79m, dolomite and intergranular pores (−). (F) Well J-174, 3128.1m, chlorite filling in pores (−). Q-quartz, TF-terrigenous feldspar, Cal-calcite, Dol-dolomite, Tu-tuff, AA-authigenic albite, Ch-chlorite, (−) represents polarized light.

**Table 1**
XRD compositions of the lacustrine fine-grained MSR in the Jimsar Sag.

| | Single fractal samples | | | Multi-fractal samples | | |
|---|---|---|---|---|---|---|
| | Min | Max | Mean | Min | Max | Mean |
| Quartz (%) | 14.4 | 22.4 | 17.9 | 15.6 | 30.3 | 24.2 |
| Total feldspar (%) | 2.1 | 44.9 | 30.9 | 11.7 | 49.8 | 31 |
| Potassium feldspar (%) | 0 | 8 | 4.2 | 0.6 | 7.9 | 4.1 |
| Plagioclase feldspar (%) | 2.1 | 41 | 26.7 | 11.1 | 44.4 | 27.2 |
| Calcite (%) | 0.5 | 22.9 | 13.3 | 0 | 12 | 2.2 |
| Dolomite (%) | 9.9 | 75.5 | 31 | 18.9 | 59.1 | 32 |
| Clay (%) | 0 | 13.9 | 8.9 | 0 | 14.8 | 9.4 |

that the enrichment of tuff in MSR can greatly improve the property and reduce the fractal dimension of pore structures through dissolution. In addition to tuff and terrigenous feldspar, a small amount of dissolution is also observed in dolomite and calcite (Fig. 10 H, I), but it has little effect on storage space.

#### 4.4.3. Cementation

Due to the close-saline depositional environment, cements in the lacustrine fine-grained MSR are mainly carbonates (dolomite and calcite) (Ding et al., 2017; Yang et al., 2019). The size of dolomite in fine-grained MSR is mainly from mud crystal to silt crystal, which relatively evenly filled in multi-scale pores (Fig. 6D and E and Fig. 10H) and reduced the reservoir storage space to a great extent. That is why the content of dolomite strongly positively correlated with fractal dimensions (Fig. 7C). Calcite in fine-grained MSR is dominated by fine to medium crystal, which mainly filled in relative macropores (Figs. 6B and 10A). Content of calcite in single fractal samples is obviously higher than that in multi-fractal samples (Table 1), leading to the former average pore-throat radius (av. 0.08 μm) is less than that of the latter (av. 0.12 μm) (Fig. 4B). Calcite reduced the storage space, but also reduced the reservoir heterogeneity to a certain extent because of its large pore filling. The high content of calcite may be one of the reasons leading to the single fractal of some samples. Thus, Compared with the increase of reservoir heterogeneity and decrease of fractal dimension by calcite cements in shale and lacustrine carbonates (Wang et al., 2015a,b; Yang et al., 2016; Xu et al., 2018), the dual influences of calcite on storage space and heterogeneity makes the weak correlation between calcite and fractal dimension in the fine-grained MSR (Fig. 7D).

Clay minerals (matrix and a small amount of authigenic clay) mainly filled in intergranular pores to reduce the storage space and increase the heterogeneity (Xiao et al., 2018), which strongly positively correlated with the fractal dimension (Fig. 7B). Though authigenic albite (Fig. 6 C, D and Fig. 10E) also filled in pores as cement, its damage to the storage space is far less than the improvement to that of the corresponding dissolution. Authigenic quartz is usually formed during the dissolution of feldspar (Wang et al., 2018b, 2019), which filled in intergranular pores and reduce the storage space (Fig. 10J).

#### 4.4.4. Dolomitization

During the burial process, the calcite was dolomitization due to the influence of $Mg^{2+}$ rich fluid (Lu et al., 2015; Wang et al., 2018b). It is common that calcite was replaced by dolomite in the fine-grained MSR, and calcite remnants are visible in the area that dolomitization was not completely (Fig. 10K). During dolomitization, the mineral crystals shrink to form a certain amount of intercrystalline pores (Fig. 10K), which can increase the storage space (Lu et al., 2015; Su et al., 2018).

#### 4.4.5. Recrystallization

Dolomite is dominated by mud crystalline in the fine-grained MSR (Fig. 6C and D). Recrystallization made mud crystalline dolomite change to microcrystalline dolomite, and then microcrystalline change to silt crystalline, leading to the dolomite grains with bigger grain size and poorer crystalline form are dispersed in the mud crystalline dolomite (Fig. 10L), which can effectively affect pore-throat structures and reduce storage spaces (Xu et al., 2018).

### 4.5. Implications of fractal characteristics on tight oil accumulation

Oiliness of the fine-grained MSR of the Lucaogou Formation in the Jimsar Sag is extremely heterogeneous (Ding et al., 2017). There are different oil-bearing grades of the fine-grained MSR, as seen in the

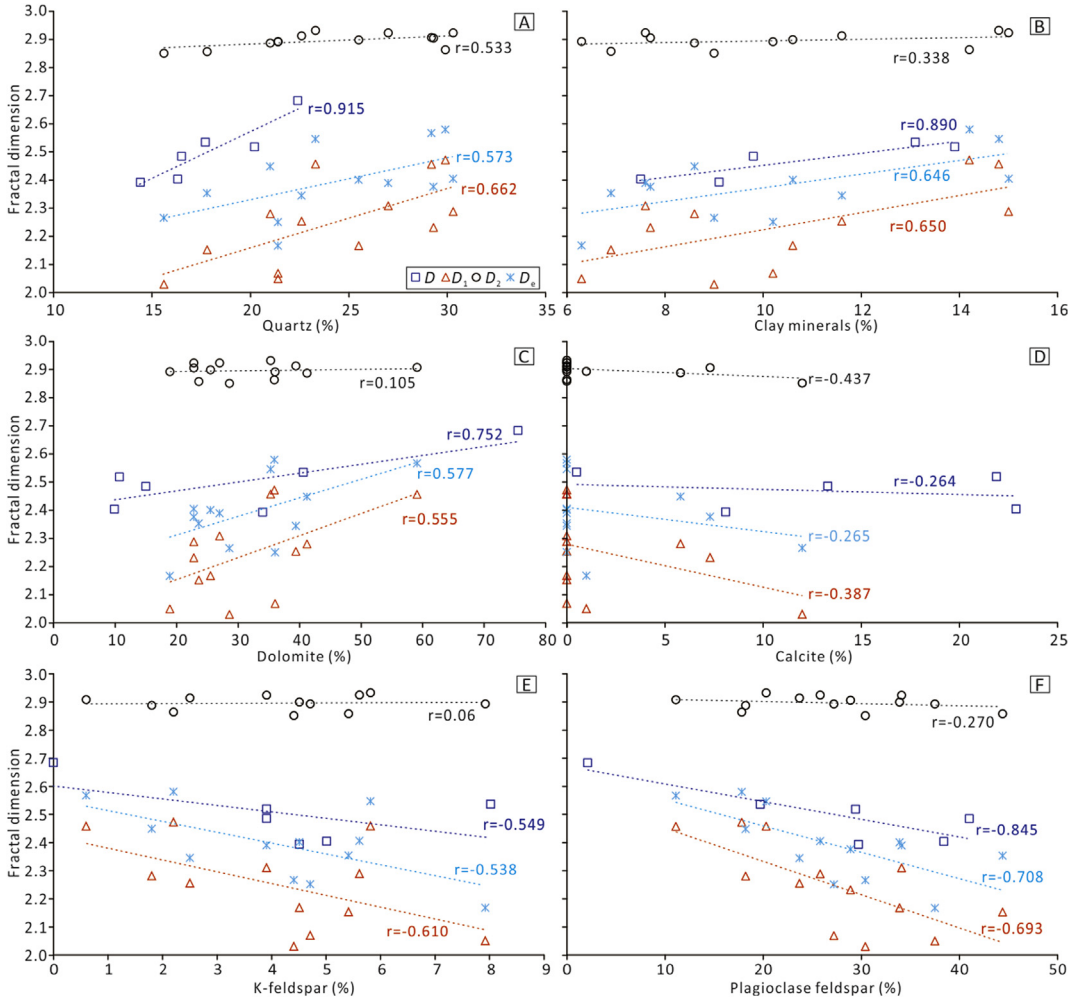


**Fig. 7.** Correlations between minerals and fractal dimensions of single and multi-fractal lacustrine fine-grained MSR samples in the Jimsar Sag.

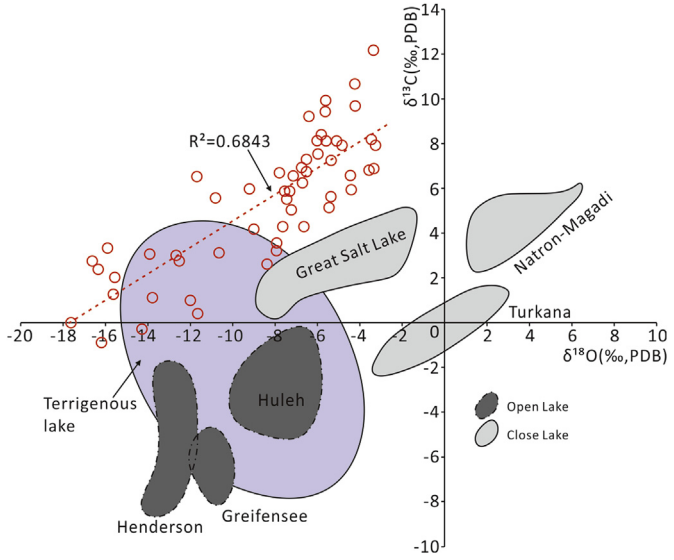


**Fig. 8.** Correlations between carbon and oxygen isotope ratios and identification of lake types of the Lucaogou Formation in the Jimsar Sag (Talbot, 1990).

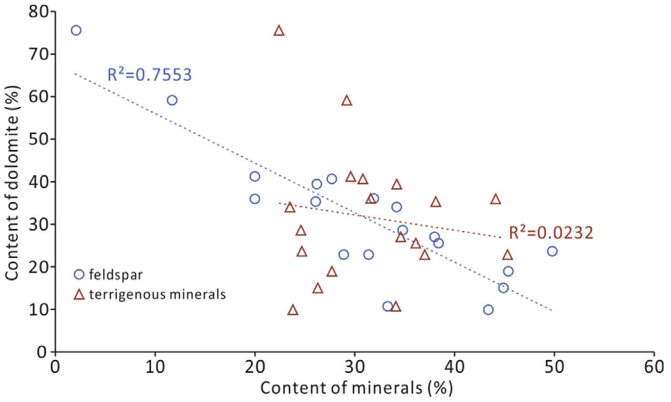


**Fig. 9.** Correlations between terrigenous minerals, feldspar and dolomite of the lacustrine fine-grained MSR in the Jimsar Sag.

cores, including fluorescence, oil trace, oil pot, oil stain. The oil content increases obviously with the changing of oil-bearing grade from fluorescence to oil stain. Compared to fluorescence samples, oil trace samples, oil potted samples and oil stained samples have apparently oil accumulation characteristics. The porosity and average pore-throat radius have positive correlations with the increase of oil content (Fig. 11A and B), and porosity and average pore-throat radius of the oil trace, oil potted and oil stained samples are obviously higher than those of fluorescence samples (Fig. 11A and B), which indicates that oil accumulation in the fine-grained MSR was obviously influenced by reservoir petrophysical properties (Zha et al., 2019; Wang et al., 2019). The reservoir petrophysical properties of the fine-grained MSR have good correlations with fractal dimensions. Samples with high porosity,

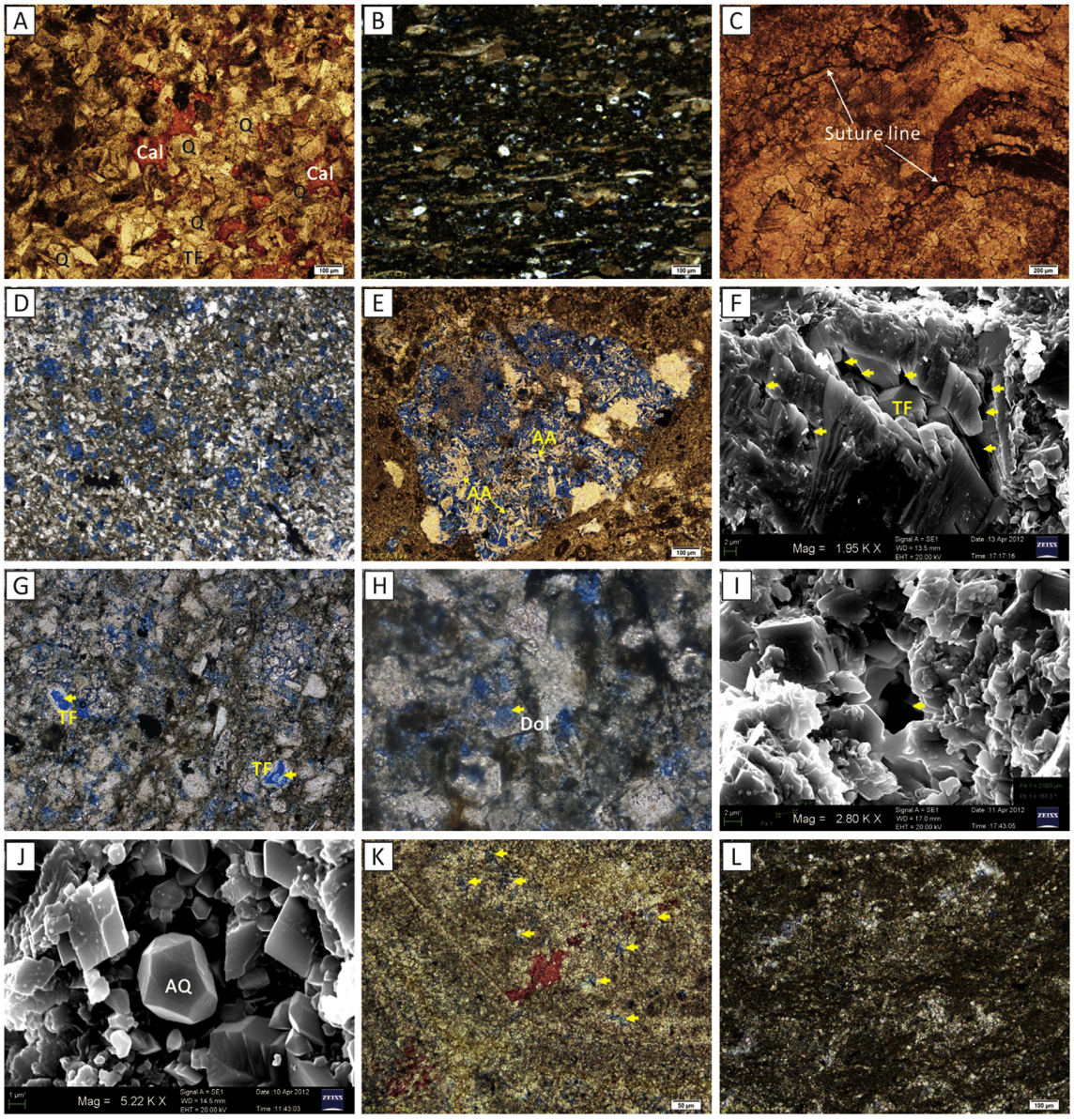


**Fig. 10.** Typical microscopic and SEM images show diagenesis of the lacustrine fine-grained MSR in the Jimsar Sag. (A) Well J-174, 3356.81m, line contact and concave-convex contact between grains and calcite cements filling in pores (−). (B) Well J-174, 3161.54m, directional arrangement of intraclast (+). (C) Well J-174, 3149.82m, suture line in carbonate component (−). (D) Well J-174, 3269.74, dissolution of tuff (−). (E) Well J-174, 3121.38m, dissolution of tuff and authigenic albite (−). (F) Well J-174, 3174.75m, dissolution of terrigenous feldspar (arrows). (G) Well J-174, 3286m, dissolution of terrigenous feldspar (arrows) (−). (H) Well J-174, 3261.23m, dissolution of dolomite (arrow) (−). (I) Well J-174, 3177.34m, intergranular dissolution of calcite (arrow). (J) Well J-174, 3121.38m, authigenic quartz filling in pores. (K) Well J-174, 3177.4m, dolomitization and intragranular pores (arrows) (−). (L) Well J-174, 3148.76m, mud-like crystal-microcrystalline dolomite recrystallized to form silt-grain dolomite plaques (−). Q-quartz, TF-terrigenous feldspar, Cal-calcite, Dol-dolomite, AA-authigenic albite, AQ-authigenic quartz, (−) represents polarized light, (+) represents perpendicular polarized light.

large pore-throat radius, good pore-throat connectivity and sorting usually have low fractal dimensions (Fig. 4). Therefore, fractal characteristics can comprehensively reflect the nanopore structures of the fine-grained MSR, and also can be discussed as the significance controlling factor for the oil accumulation. The fractal dimensions decrease with the increase content of oil and the fractal dimensions of the oil trace, oil potted and oil stained samples are obviously lower than those of fluorescence samples also indicate the controls of fractal characteristics on the tight oil accumulation (Fig. 11C).

The oil-bearing grade has good correlations with the content of different types of minerals (Fig. 12). The quartz and carbonate contents gradually decrease and the feldspar content gradually increases with the increasing content of oil (Fig. 12). The clay content of the oil trace, oil potted and oil stained samples is obviously lower than that of fluorescence samples (Fig. 12). As discussed above, in the fine-grained MSR, the quartz, clay and carbonate can reduce the storage space and increase the heterogeneity of pore structures through compaction, cementation and recrystallization, whereas the feldspar indicates the strong dissolution and is favorable to improve reservoir petrophysical properties. Therefore, the decrease of quartz, clay and carbonate content and enrichment of feldspar are favorable for oil accumulation in the fine-grained MSR. Fractal dimensions are not only the response of reservoir petrophysical properties, but also can effectively reflect the content of minerals of the fine-grained, MSR (Fig. 7). Therefore, the influences of minerals on tight oil accumulation can also be described by the fractal dimensions.

In summary, fractal characteristics can comprehensively reflect reservoir properties and mineral composition, and play a very important

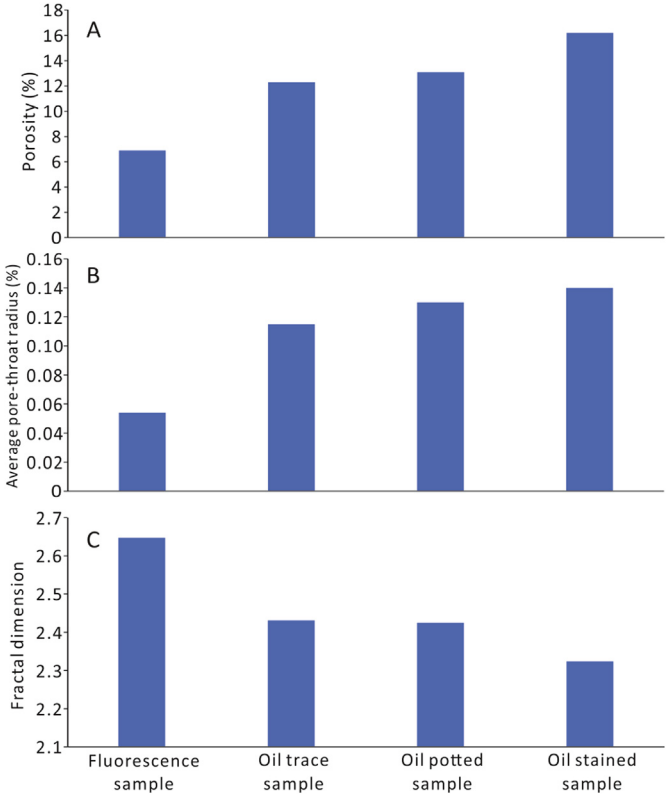


**Fig. 11.** Correlations of oil-bearing grade with porosity, average pore-throat radius and fractal dimension of the fine-grained MSR of the Lucaogou Formation in the Jimsar Sag. Fractal dimension of multi-fractal samples is using the $D_e$.

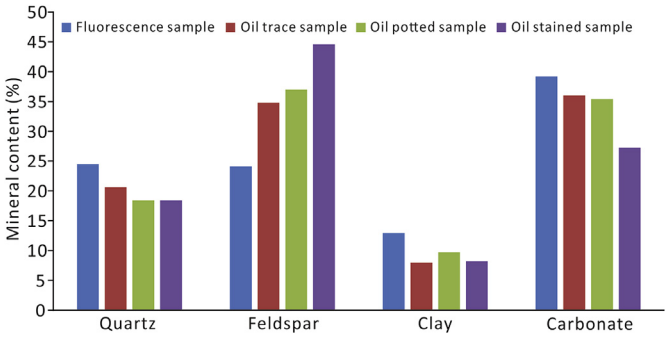


**Fig. 12.** Correlations of oil-bearing grade with contents of different types of minerals of the fine-grained MSR of the Lucaogou Formation in the Jimsar Sag.

role in controlling the accumulation of tight oil in the fine-grained MSR. There is an upper limit for the fractal dimension defines ability to accumulate oil. The fractal dimension vs. porosity and fractal dimension vs. average pore-throat radius plots indicate that the upper limit of the fractal dimension and the lower limits of porosity and average pore-throat radius for apparently accumulating oil are 2.586, 6.3% and 0.05 μm, respectively (Fig. 13). Fine-grained MSR with fractal dimension more than the limit, and porosity or average pore-throat radius less than the limits did not effectively accumulate oil.

## 5. Conclusions

(1) The pore structures of the lacustrine fine-grained MSR tight oil reservoirs are characterized by single and multi-fractal structures. Compared with the multi-fractal reservoir, the pore-throat structure of single fractal reservoir is more uniform and the pore throat size is relatively smaller. For multi-fractal reservoir, the heterogeneity of large pores is obviously stronger than that of small pores because of the low content and poor connectivity.

(2) Minerals and diagenesis have apparent influences on fractal characteristics of the lacustrine fine-grained MSR tight oil reservoir. The enrichment of terrestrial minerals can increase the heterogeneity of storage space and might be the reason for the multi-fractal pore structures. The enrichment of tuff in fine-grained MSR can greatly improve the property and reduce the fractal dimension of tight reservoirs through dissolution. Large-pore filling calcite has dual effects on destroying reservoir space and reducing heterogeneity, which makes the weak correlation between calcite and fractal dimension.

(3) Fractal characteristics of pore structures play a very important role in controlling the accumulation of tight oil. There is an upper limit of fractal dimension for accumulation of tight oil in the fine-grained MSR reservoir.

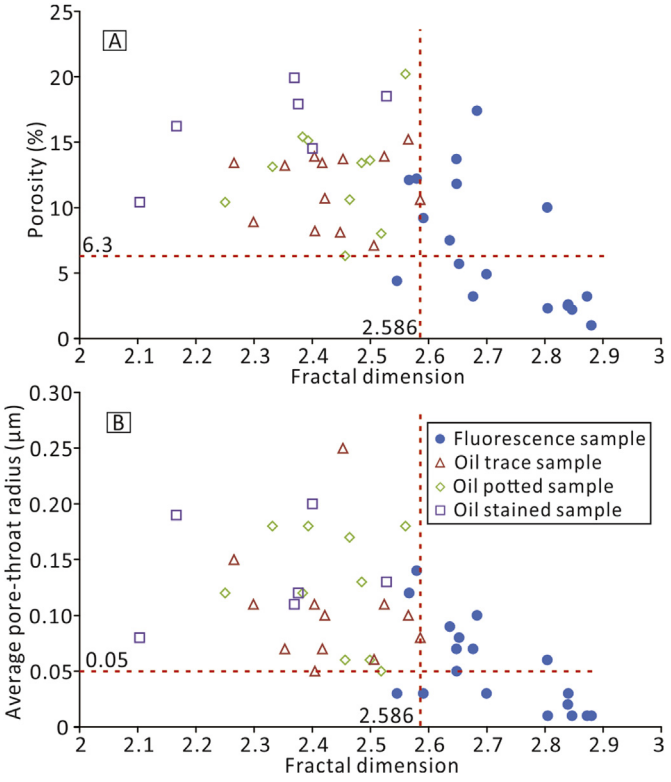


**Fig. 13.** Fractal dimension vs. porosity and fractal dimension vs. average pore-throat radius plots of samples with different oil-bearing grades of the fine-grained MSR of the Lucaogou Formation in the Jimsar Sag. Fractal dimension of multi-fractal samples is using the $D_e$.

## Acknowledgments

This work was co-funded by the Shandong Provincial Natural Science Foundation (ZR2019MD004), the National Natural Science Foundation of China (Grant No. U1762217, 418210002), the Fundamental Research Funds for the Central Universities (18CX05027A, 16CX02027A), the National Science and Technology Special of China (2017ZX05009001), and the Strategic Priority Research Program of the Chinese Academy of Sciences (Grant No. XDA14010301). We are grateful to the Research Institute of Petroleum Exploration and Development, PetroChina Xinjiang Oilfield, for permission to access their in-house database, providing background geologic data and permission to publish the results.

## Appendix A. Supplementary data

Supplementary data to this article can be found online at https://doi.org/10.1016/j.petrol.2019.106363.

## References


Al-Asam, I.S., Taylor, B.E., South, B., 1990. Stable isotope analysis of multiple carbonate samples using selective acid extraction. Chem. Geol. 80, 119–125.

Anovitz, L.M., Cole, D.R., Rother, G., Allard, L.F., Jackson, A.J., Littrell, K.C., 2013. Diagenetic changes in macro to nano-scale porosity in the St. Peter Sandstone: an (ultra) small angle neutron scattering and backscattered electron imaging analysis. Geochem. Cosmochim. Acta 102, 280–305.

Bai, B., Zhu, R., Wu, S., Yang, W., Jeff, G., Allen, G., et al., 2013. Multiscale method of nano (micro)-CT study on microscopic pore structure of tight sandstone of Yanchang Formation, Ordos Basin. Pet. Explor. Develop. 40, 354–358.

Barnard, S., Wirth, R., Schreiber, A., Schulz, I.M., Horsfield, B., 2012. formation of nanoporous pyrobitumen residues during maturation of the Barnett shale (Forth Worth basin). Int. J. Coal Geol. 103, 3–11.

Cao, T., Song, Z., Wang, S., Xia, J., 2016a. Characterization of pore structure and fractal dimension of Paleozoic shales from the northeastern Sichuan Basin, China. Nat. Gas Sci. Eng. 35, 882–895.

Cao, Z., Liu, G., Kong, Y., Wang, C., Niu, Z., Zhang, J., Geng, C., Shan, X., Wei, Z., 2016b. Lacustrine tight oil accumulation characteristics: permian Lucaogou Formation in Jimusaer sag, Junggar Basin. Int. J. Coal Geol. 153, 37–51.

Carr, M.B., Ehrlich, R., Bowers, M.C., Howard, J.J., 1996. Correlation of porosity types derived from NMR data and thin section image analysis in a carbonate reservoir. J. Pet. Sci. Eng. 14, 115–131.

Chalmers, G.R.L., Bustin, R.M., Power, I.M., 2012. Characterization of gas shale pore systems by porosimetry, pycnometry, surface area, and field emission scanning electron microscopy/transmission electron microscopy image analyses: examples from the Barnett, Woodford, Haynesville, Marcellus, and Doig units. AAPG Bull. 96, 1099–1119.

Chen, Q., Zhang, J., Tang, X., Li, W., Li, Z., 2016. Relationship between pore type and pore size of marine shale: an example from the Sinian–Cambrian formation, upper Yangtze region, South China. Int. J. Coal Geol. 158, 13–28.

Curtis, M.E., Cardott, B.J., Sondergeld, C.H., 2012. Development of organic porosity in the Woodford Shale with increasing thermal maturity. Int. J. Coal Geol. 103, 26–31.

Clarkson, C.R., Freeman, M., He, L., Agamalian, M., Melnichenko, M., Mastalerz, M., et al., 2012. Characterization of tight gas reservoir pore structure using USANS/SANS and gas adsorption analysis. Fuel 95, 371–385.

Clarkson, C.R., Solano, N., Bustin, R.M., Bustin, A.M.M., Chalmers, G.R.L., He, L., et al., 2013. Pore structure characterization of North American shale gas reservoirs using USANS/SANs, gas adsorption, and mercury intrusion. Fuel 103, 606–616.

Dathe, A., Eins, S., Niemeyer, J., Gerold, G., 2001. The surface fractal dimension of the soil–pore interface as measured by image analysis. Geoderma 103, 203–229.

Ding, X., Gao, C., Zha, M., Chen, H., Su, Y., 2017. Depositional environment and factors controlling β-carotane accumulation: a case study from the Jimsar Sag, Junggar Basin, northwestern China. Palaeogeogr. Palaeoclimatol. Palaeoecol. 485, 833–842.

Fu, H., Tang, D., Xu, T., Xu, H., Tao, S., Li, S., et al., 2017. Characteristics of pore structure and fractal dimension of low-rank coal: a case study of Lower Jurassic Xishanyao coal in the southern Junggar Basin, NW China. Fuel 193, 254–264.

Ghanizadeh, G., Clarkson, C.R., Aquino, S., Ardakani, O.H., Sane, H., 2015. Petrophysical and geomechanical characteristics of Canadian tight oil and liquid-rich gas reservoirs: I. Pore network and permeability characterization. Fuel 153, 664–681.

Jaroniec, M., 1995. Evaluation of the fractal dimension from a single adsorption isotherm. Langmuir 11, 2316–2317.

Ji, W., Song, Y., Jiang, Z., Meng, M., Liu, Q., Chen, L., et al., 2016. Fractal characteristics of nano-pores in the lower Silurian Longmaxi shales from the upper Yangtze Platform, south China. Mar. Pet. Geol. 78, 88–98.

Keith, M.L., Weber, J.N., 1964. Carbon and oxygen isotopic composition of selected limestones and fossils. Geochem. Cosmochim. Acta 28, 1787–1816.

Krohn, C.E., 1988. Sandstone fractal and euclidean pore volume distributions. Geophys. Res. 93, 3286–3296.

Lai, J., Wang, G., 2015. Fractal analysis of tight gas sandstones using high-pressure mercury intrusion techniques. J. Nat. Gas Sci. Eng. 24, 185–196.

Li, P., Zheng, M., Bi, H., Wu, S., Wang, X., 2017. Pore throat structure and fractal characteristics of tight oil sandstone: a case study in the Ordos Basin, China. J. Pet. Sci. Eng. 149, 665–674.

Li, Y., Tang, D., Elsworth, D., Xu, H., 2014. Characterization of coalbed methane reservoirs at multiple length scales: a cross-section from southeastern Ordos basin, China. Energy Fuels 28, 5587–5595.

Loucks, R.G., Reed, R.M., Ruppel, S.C., 2009. Morphology, genesis, and distribution of nanometer-scale pores in siliceous mudstones of the Mississippian Barnett shale. J. Sediment. Res. 79, 848–861.

Loucks, R.G., Ruppel, S.C., Wang, X., Ko, L., Peng, S., Zhang, T., et al., 2017. Pore types, pore-network analysis, and pore quantification of the lacustrine shale-hydrocarbon system in the Late Triassic Yanchang Formation in the southeastern Ordos Basin, China. Interpretation 5, SF63–SF79.

Lu, X., Shi, J., Zhang, S., Zou, N., Sun, G., Zhang, S., 2015. The origin and formation model of Permian dolostones on the northwestern margin of Junggar Basin, China. J. Asian Earth Sci. 105, 456–467.

Mahamud, M.M., Novo, M.F., 2008. The use of fractal analysis in the textural characterization of coals. Fuel 87, 222–231.

Ma, J., Huang, Z., Gao, X., Chen, C., 2015. Oil-source rock correlation for tight in tuffaceous reservoirs in the Permian Tiaohu Formation, Santanghu Basin, northwest China. Can. J. Earth Sci. 52, 1014–1026.

Ma, J., Huang, Z., Li, T., 2019. Mechanism of hydrocarbon accumulation and enrichment of tuffaceous tight oil with separate reservoir and source rock: a case study of tuff reservoir from the Permian Tiaohu Formation in the Santanghu Basin, northwest China. AAPG Bull. 103, 345–367.

Ma, K., Hou, J., Yan, L., Chen, F., 2018. Pore-throat structures and their control of terrestrial lacustrine tight reservoir quality: the Permian Lucaogou Formation, Jimsar Sag, northwestern China. Interpretation 6, T889–T906.

Mandelbrot, B.B., Passoja, D.E., Paullay, D.E., 1984. Fractal character of fracture surfaces in porous media. Nature 308, 721–722.

Mastalerz, M., Schimmelmann, A., Drobniak, A., Chen, Y., 2013. Porosity of Devonian and Mississippian New Albany shale across a maturation gradient: insights from organic petrology, gas adsorption, and mercury intrusion. AAPG Bull. 97, 1621–1643.

Mendhe, V.A., Bannerjee, M., Varma, A.K., Kamble, A.D., Mishra, S., Singh, B.D., 2017. Fractal and pore dispositions of coal seams with significance to coalbed methane plays of East Bokaro, Jharkhand, India. J. Nat. Gas Sci. Eng. 38, 412–433.

Myrow, P.M., Landing, E., 1992. Mixed siliciclastic-carbonate deposition in an Early Cambrian oxygen-stratified basin, Chapel Island Formation, southeastern Newfoundland. J. Sediment. Res. 62, 455–473.

Palermo, D., Aigner, T., Geluk, M., Poeppelreiter, M., Pipping, K., 2008. Reservoir potential of a lacustrine mixed carbonate/siliciclastic gas reservoir: the Lower Triassic rogenstein in The Netherlands. J. Pet. Geol. 31, 61–96.

Pfeifer, P., Avnir, D.J., 1983. Chemistry in noninteger dimensions between two and three. I. Fractal theory of heterogeneous surfaces. J. Chem. Phys. 79, 3558–3565.

Pfeifer, P., Wu, Y., Cole, M., Krim, J., 1989. Multilayer adsorption on a fractally rough surface. Phys. Rev. Lett. 62, 1997.

Schieber, J., 2010. Common themes in the formation and preservation of intrinsic porosity in shales and mudstone-illustrated with examples across the Phanerozoic. In: Society of Petroleum Engineers Unconventional Gas Conference, Pittsburgh, Pennsylvania, SPE Paper, vol. 13270. pp. 12.

Shanley, K.W., Cluff, R.M., 2015. The evolution of porescale fluid-saturation in low-permeability sandstone reservoirs. AAPG Bull. 99, 1957–1990.

Sharawy, M.S.E., Gaafar, G.R., 2019. Pore-Throat size distribution indices and their relationships with the petrophysical properties of conventional and unconventional clastic reservoirs. Mar. Pet. Geol. 99, 122–134.

Shao, X., Pang, X., Li, Q., Wang, P., Chen, D., Shen, W., et al., 2017. Pore structure and fractal characteristics of organic-rich shales: a case study of the lower Silurian Longmaxi shales in the Sichuan Basin, SW China. Mar. Pet. Geol. 80, 192–202.

Su, Y., Zha, M., Ding, X., Qu, J., Wang, X., Yang, C., 2018. Pore type and pore size distribution of tight reservoirs in the permian Lucaogou Formation of the Jimsar sag, Junggar Basin, NW China. Mar. Pet. Geol. 89, 761–774.

Talbot, M.R., 1990. A review of the palaeohydrological interpretation of carbon and oxygen isotopic ratios in primary lacustrine carbonates. Chem. Geol. 80, 261–279.

Tao, K., Cao, J., Wang, Y., Ma, W., Xiang, B., Ren, J., Zhou, N., 2016. Geochemistry and origin of natural gas in the petroliferous Mahu sag, northwestern Junggar Basin, NW China: Carboniferous marine and Permian lacustrine gas systems. Org. Geochem. 100, 62–79.

Wang, J., Cao, Y., Liu, K., Liu, J., Xue, X., Xu, Q., 2016. Pore fluid evolution, distribution and water-rock interactions of carbonate cements in red-bed sandstone reservoirs in the Dongying Depression, China. Mar. Pet. Geol. 72, 279–294.

Wang, J., Cao, Y., Liu, K., Costanzo, A., Feely, M., 2018b. Diagenesis and evolution of the lower Eocene red-bed sandstone reservoirs in the Dongying Depression, China. Mar. Pet. Geol. 94, 230–245.

Wang, J., Cao, Y., Wang, X., Liu, K., Wang, Z., Xu, Q., 2018c. Sedimentological constraints on the initial uplift of the west Bogda Mountains in Mid-Permian. Sci. Rep. 8, 1453.

Wang, J., Cao, Y., Xiao, J., Liu, K., Song, M., 2019. Factors controlling reservoir properties and hydrocarbon accumulation of the Eocene lacustrine beach-bar sandstones in the Dongying Depression, Bohai Bay Basin, China. Mar. Pet. Geol. 99, 1–16.

Wang, M., Xue, H., Tian, S., Wilkins, R.W., Wang, Z., 2015a. Fractal characteristics of upper Cretaceous lacustrine shale from the Songliao basin, NE China. Mar. Pet. Geol. 67, 144–153.

Wang, W., Shahvali, M., Su, Y., 2015b. A semi-analytical fractal model for production from tight oil reservoirs with hydraulically fractured horizontal wells. Fuel 158, 612–618.

Wang, X., Hou, J., Wang, D., Gong, L., Ma, K., Liu, Y., et al., 2018a. Combining pressure-controlled porosimetry and rate-controlled porosimetry to investigate the fractal characteristics of full-range pores in tight oil reservoirs. J. Pet. Sci. Eng. 171, 353–361.

Wei, W., Zhu, X., Zhu, S., He, M., Wu, J., Wang, M., 2017. Lithofacies and reservoir space characteristics of the tuffaceous-siliciclastic mixed rocks of the lower Cretaceous Tenggeer Formation in anan sag, Erlian Basin. Lit. Res. 29, 68–76 (in Chinese with English abstract).

Wu, H., Hu, W., Cao, J., Wang, X., Liao, Z., 2016. A unique lacustrine mixed dolomitic-clastic sequence for tight oil reservoir within the middle Permian Lucaogou Formation of Junggar Basin, NW China: reservoir characteristics and origin. Mar. Pet. Geol. 76, 115–132.

Xiao, D., Jiang, S., Thul, D., Lu, S., Zhang, L., Lia, B., 2018. Impacts of clay on pore structure, storage and percolation of tight sandstones from the Songliao Basin, China: implications for genetic classification of tight sandstone reservoirs. Fuel 211, 390–404.

Xu, Q., Ma, Y., Liu, B., Song, X., Li, L., Xu, J., et al., 2018. Fractal characteristics of lacustrine tight carbonate nanoscale reservoirs. Energy Fuels 32, 107–118.

Yang, R., He, S., Yi, J., Hu, Q., 2016. Pore characterization and methane sorption capacity of over-mature organic-rich Wufeng and Longmaxi shales in the southeast Sichuan

Basin, China. Mar. Pet. Geol. 70, 27–45.
Yang, Y., Qiu, L., Wan, M., Jia, X., Cao, Y., Lei, D., et al., 2019. Depositional model for a salinized lacustrine basin: the permian Lucaogou Formation, Jimsar sag, Junggar Basin, NW China. J. Asian Earth Sci. 178, 81–95.
Zha, M., Wang, S., Ding, X., Feng, Q., Xue, H., Su, Y., 2019. Tight oil accumulation mechanisms of the Lucaogou Formation in the Jimsar Sag, NW China: insights from pore network modeling and physical experiments. J. Asian Earth Sci. 178, 204–215.
Zhao, H., Ning, Z., Wang, Q., Zhang, R., Zhao, T., Niu, T., et al., 2015. Petrophysical characterization of tight reservoirs using pressure-controlled porosimetry combined with rate-controlled porosimetry. Fuel 154, 233–242.
Zhou, S., Liu, D., Cai, Y., Yao, Y., 2016. Fractal characterization of pore–fracture in low-rank coals using a low-field NMR relaxation method. Fuel 181, 218–226.
Zou, C., Zhu, R., Liu, K., Su, L., Bai, B., Zhang, X., et al., 2012. Tight gas sandstone reservoirs in China: characteristics and recognition criteria. J. Pet. Sci. Eng. 88, 82–91.
Zou, C., Zhang, G., Yang, Z., Tao, S., Hou, L., Zhu, R., et al., 2013. Geological concepts, characteristics, resource potential and key techniques of unconventional hydrocarbon:On unconventional petroleum geology. Pet. Explor. Dev. 40, 385–399.